CrossMark

RESEARCH ARTICLE

Investigation on terahertz generation from zinc-blende crystal waveguide at polariton resonance

Zhongyang Li[1] · **Mengtao Wang**[1] · **Silei Wang**[1] · **Pibin Bing**[1] · **Sheng Yuan**[1]

Abstract Terahertz (THz) wave generation from zinc-blende crystal waveguide, such as GaAs, InP, ZnTe and CdTe, at polariton resonance region (PRR) with a transverse pumping geometry is investigated. It is shown that by using grating vector of periodically inverted crystal, THz wave can be efficiently generated by difference frequency generation (DFG) with a transverse pumping geometry. Parametric gain coefficients in the low-loss limit and absorption coefficients of THz wave during DFG process in the vicinity of PRR are analyzed. The frequency tuning characteristics of THz wave via varying wavelength of difference frequency waves and poling period of periodically inverted crystal are numerically analyzed.

Keywords Terahertz wave · Difference frequency generation · Zinc-blende crystal · Transverse pumping geometry

Introduction

In the research of modern terahertz (THz) optoelectronics, monochromatic THz sources play an important role in high-resolution THz applications, such as environmental gas monitoring, high-density and high-speed wireless communications [1–4]. Difference frequency generation (DFG) with two closely spaced laser frequencies ω_1 and ω_2 in second-order nonlinear optics crystals is one of the promising processes for efficient monochromatic THz wave output in the wide frequency tuning range and room temperature operation [5, 6]. THz wave generation based on DFG has been intensively researched [7–9]. Unfortunately, the maximum frequencies generated by these optics processes are limited to 7 THz [10]. Moreover, the output power of THz wave with high frequency is extremely low. Such limitations on output frequencies and power are caused by the dramatically increased absorption of the nonlinear materials in the vicinity of polariton resonance region (PRR). However, at the same time, polariton resonances can induce giant second-order nonlinearities. The giant second-order nonlinearities in the vicinity of PRR can be exploited to extend the output frequencies and enhance the output power of THz wave [11]. In the vicinity of PRR for THz wave generation, the crucial point for efficient THz wave generation is to minimize the path of THz wave in the crystal. A transverse pumping geometry can overcome this problem [12–14]. The optical beams propagate close to crystal lateral surface, and THz wave radiates from the crystal surface and propagates perpendicular to the direction of the optical beams. The absorption loss is minimized because the THz wave is generated from the crystal surface.

A frequently employed material for DFG is the nonlinear optical crystal MgO:LiNbO$_3$, because of its relatively large second-order nonlinear optical coefficient ($d_{33} = 25.0$ pm/V at 1064 nm) and its wide transparency range [15]. However, DFG from zinc-blende-type semiconductors, such as GaP, GaAs and CdTe, is advantageous in obtaining an intense THz wave since their second-order nonlinear optical coefficients are several times larger than that of MgO:LiNbO$_3$. d_{36} of GaAs, GaP and CdTe is 170 pm/V, 70.6 pm/V and 109 pm/V at 1064 nm, respectively [16, 17]. In addition, their absorption coefficients in

✉ Zhongyang Li
 thzwave@163.com

1 College of Electric Power, North China University of Water Resources and Electric Power, Zhengzhou 450045, Henan, China

the THz frequency region are about ten times smaller than that of MgO:LiNbO$_3$ [18].

In this paper, we explore THz wave generation from zinc-blende crystals, such as GaAs, InP, ZnTe and CdTe with a transverse pumping geometry. Parametric gain coefficient in the low-loss limit of THz wave during DFG process in the vicinity of PRR is analyzed. We investigate the frequency tuning characteristics of THz wave via varying wavelength of optical waves and poling period of periodically inverted crystal.

Theoretical model

The schematic drawing of a surface-emitted DFG from zinc-blende crystal waveguide with a transverse pumping geometry is presented in Fig. 1. Two input optical waves λ_1 and λ_2 at the frequencies of ω_1 and ω_2 in the infrared (IR) domain are propagating collinear along the x-axis in a zinc-blende crystal waveguide. The waveguide is achieved by periodically switching the orientation between [111] and [$\bar{1}\bar{1}\bar{1}$], achievable through the epitaxial growth of zinc-blende crystals on an orientation-patterned substrate [19, 20]. A THz wave is emitted due to the oscillating nonlinear polarization at the difference frequency between the two input waves. The radiation angle θ between directions of the optical and THz wave propagation is determined by the refractive index of optical waves and THz wave in the crystal, and the poling period of periodically inverted crystal,

$$\cos\theta = \frac{K_{IR}}{K_{THz}}, \tag{1}$$

where $K_{THz} = \omega_{THz} n_{THz}/c$ is the wave vector of THz wave, n_{THz} is the refractive index at ω_{THz} frequency; $K_{IR} = n_1\omega_1/c - n_2\omega_2/c - 2\pi/\Lambda$, where Λ is the poling period of periodically inverted crystal, n_1 and n_2 are the refractive indices at optical wavelengths λ_1 and λ_2 at ω_1 and ω_2 frequencies, respectively. THz wave can be generated in a direction perpendicular to the optical wave propagations if K_{IR} equals to zero.
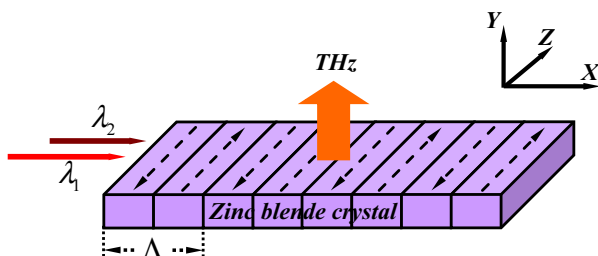
The parametric gain coefficient g_0 in the low-loss limit during DFG processes in cgs units can be determined by the following expression [21]:

$$g_0^2 = \frac{\pi\omega_{THz}\omega_2}{2c^3 n_1 n_2 n_{THz}} I_{\lambda 1} \left(d'_E + \frac{S\omega_0^2 d'_Q}{\omega_0^2 - \omega_{THz}^2} \right)^2 \tag{2}$$

$$\alpha_{THz} = 2\frac{\omega_{THz}}{c} \operatorname{Im}\left(\varepsilon_\infty + \frac{S\omega_0^2}{\omega_0^2 - \omega_{THz}^2 - i\omega_{THz}\Gamma} \right)^{\frac{1}{2}} \tag{3}$$

where α_{THz} is absorption coefficient in THz region, and ω_0, S and Γ denote eigen frequency, oscillator strength of the polariton mode and the bandwidth of the phonon mode in the zinc-blende crystal, respectively. $I_{\lambda 1}$ is the power density of the optical wave with wavelength λ_1. d'_E and d'_Q are nonlinear coefficients related to pure parametric (second order) and Raman (third order) scattering processes, respectively. The relationship between d'_E and d'_Q is [21].

$$d'_E + Sd'_Q = rn_1^4 \tag{4}$$

where r is the electro-optic coefficient. In this paper, the data for GaAs, InP, ZnTe and CdTe are taken from references [16, 22, 23].

Parametric gain characteristics

GaAs, InP, ZnTe and CdTe have infrared- and Raman-active transverse optical (TO) phonon modes at the frequencies of 269 cm^{-1}, 304 cm^{-1}, 179 cm^{-1} and 141 cm^{-1}, respectively. The TO phonon modes are useful for efficient THz wave generation because of the largest parametric gain in the vicinity of PRR, as shown in Fig. 2. From the figure, we find that the central frequencies of PRR are 4.23 THz, 5.37 THz, 8.07 THz and 9.12 THz, corresponding to CdTe, ZnTe, GaAs and InP, respectively. As THz wave frequencies approach PRR, the parametric gain coefficient g_0 sharply reaches a maximum value ($> 10^5$ cm^{-1}) and the absorption coefficient α_{THz} intensively increases to 10^4 cm^{-1}. Such dramatic enhancements of parametric gain coefficients can be exploited for improving the output powers and extending the frequency bands of THz waves if using a transverse pumping geometry to minimize the propagation path of THz wave within the crystal. As discussed above, output frequencies of THz wave from 4.23 THz to 9.12 THz can be efficiently realized in the vicinity of PRR by using CdTe, ZnTe, GaAs and InP with a transverse pumping geometry.
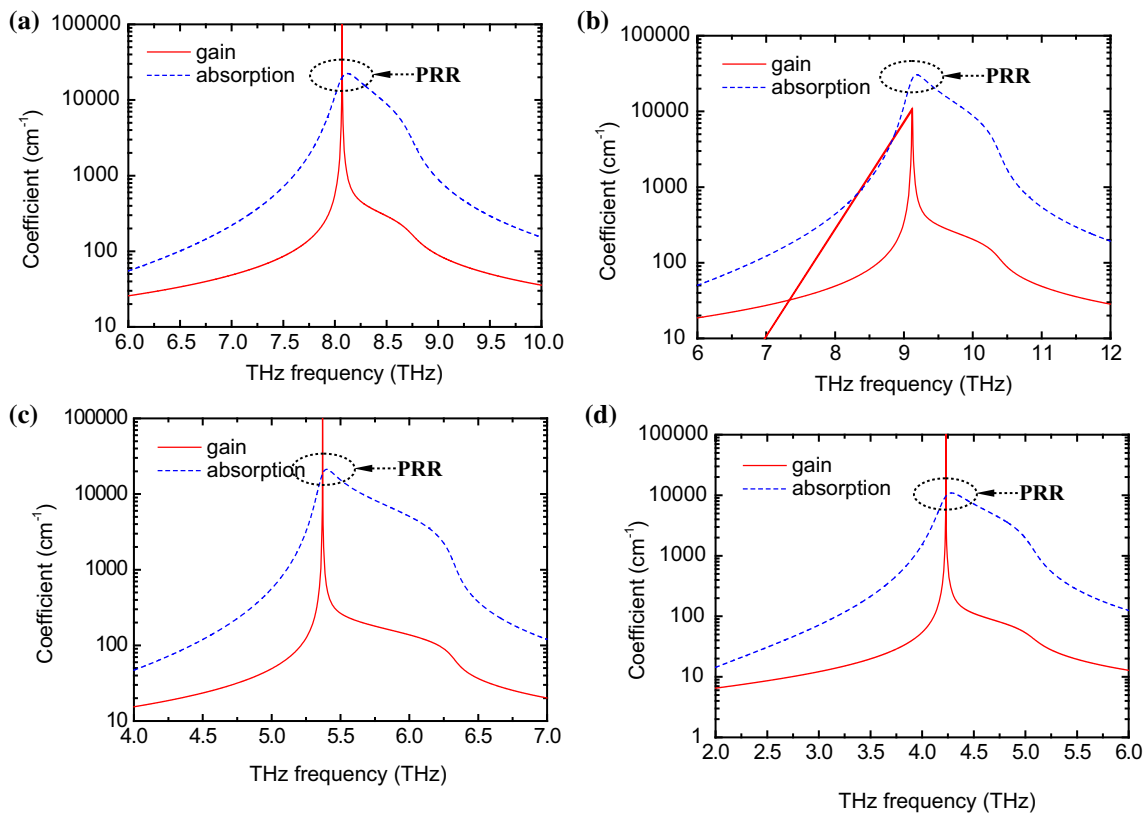

Fig. 1 Schematic diagram of a surface-emitted DFG from zinc-blende crystal waveguide with a transverse pumping geometry

Fig. 2 Parametric gain coefficient in the low-loss limit g_0 and absorption coefficient α_{THz} versus THz wave frequency at room temperature. $\lambda_1 = 1.064$ μm, $I_{\lambda 1} = 100$ MW/cm^2. **a** GaAs, **b** InP, **c** ZnTe, **d** CdTe

Frequency tuning characteristics

According to Eq. (1), the frequencies of the THz wave can be tuned by varying poling period Λ and wavelength of optical waves λ_1 and λ_2. Figure 3 shows the tuning characteristics as a function of optical wavelength λ_1 ranging from 0.75 to 2.5 μm. From the figure, we find that the frequencies of THz wave are rapidly and smoothly increased with the increase in wavelength λ_1. In Fig. 3a, THz wave with frequencies ranging from 5.65 to 8.88 THz can be obtained from GaAs crystal as $\Lambda = 10$ μm. The central frequency of PRR corresponds to $\lambda_1 = 1.22$ μm. Similarly, THz wave with frequencies ranging from 8.25 to 9.62 THz, from 4.71 to 5.76 THz and from 3.22 to 7.29 THz can be obtained from InP, ZnTe and CdTe crystals as $\Lambda = 10$ μm, $\Lambda = 20$ μm and $\Lambda = 15$ μm, respectively. The central frequency of PRR corresponds to $\lambda_1 = 1.08$ μm, $\lambda_1 = 1.13$ μm and $\lambda_1 = 0.8$ μm, respectively. THz wave generated from PRR can be realized by tuning the wavelength λ_1.

The frequencies of THz wave as a function of poling period Λ as $\lambda_1 = 1.064$ μm are depicted in Fig. 4. From the figure, we find that widely tunable THz wave can be obtained by varying poling period Λ. From the figure, we

find that the frequencies of THz wave are rapidly and smoothly decreased with the increase in poling period Λ. As shown in Fig. 4a, b, THz wave with frequencies ranging from 9.5 to 1.6 THz and from 11.3 to 1.9 THz can be obtained from GaAs and InP crystals as Λ changes from 8 to 48 μm, respectively. The central frequencies of PRR correspond to $\Lambda = 9.4$ μm and $\Lambda = 9.9$ μm, respectively. As shown in Fig. 4c, d, THz wave with frequencies ranging from 10.5 to 2.1 THz and from 9.4 to 1.88 THz can be obtained from ZnTe and CdTe crystals as Λ changes from 10 to 50 μm, respectively. The central frequencies of PRR correspond to $\Lambda = 19.7$ μm and $\Lambda = 22.1$ μm, respectively. THz wave generated from PRR can realized by tuning the poling period Λ.

Compared with other works in which THz wave generations are far from PRR to avoid intensive absorption, the theoretical model proposed in this letter can exploit dramatic enhancement of parametric gain in the vicinity of PRR with a transverse pumping geometry. The theoretical model proposed in this work is useful to other materials with crystal birefringence properties, such as LiNbO$_3$, LiTaO$_3$ and KTA, in which polaritons are both infrared active and Raman active. The theoretical model is also useful to semiconductor optical waveguide with modal birefringence properties. By utilizing modal birefringence
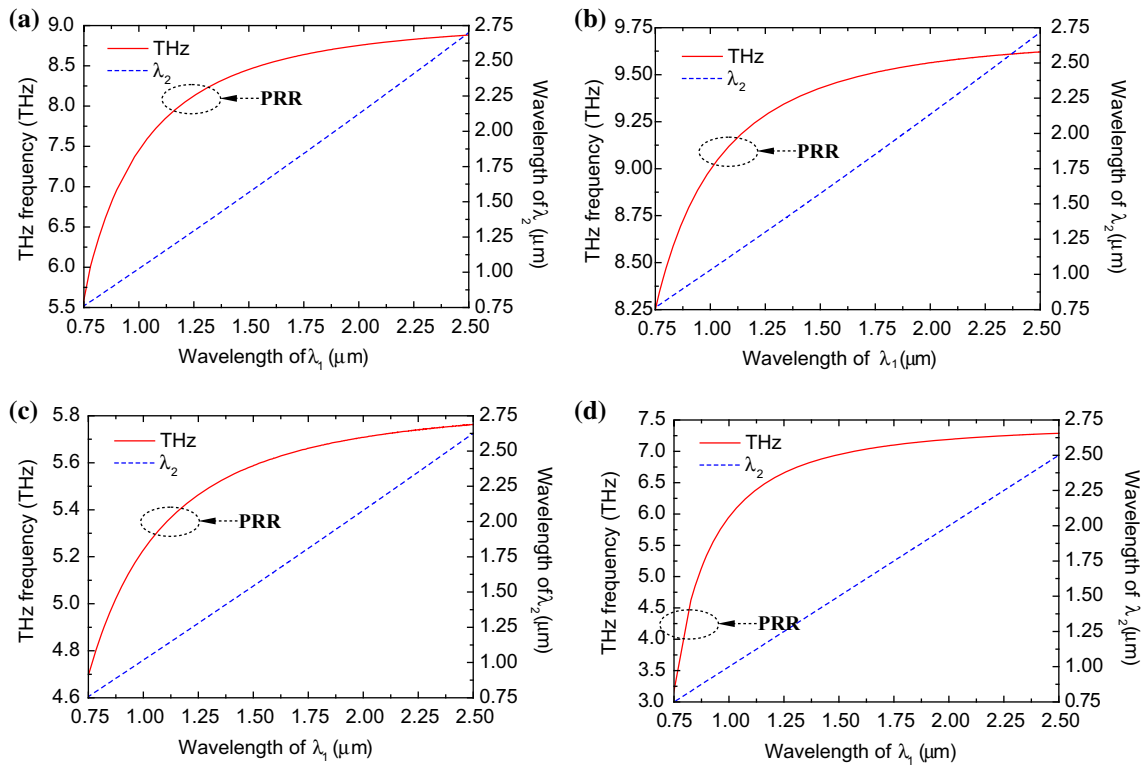
Fig. 3 THz wave frequencies versus the wavelength of optical wave λ_1. **a** GaAs, $\Lambda = 10$ μm, **b** InP, $\Lambda = 10$ μm, **c** ZnTe, $\Lambda = 20$ μm, **d** CdTe, $\Lambda = 15$ μm
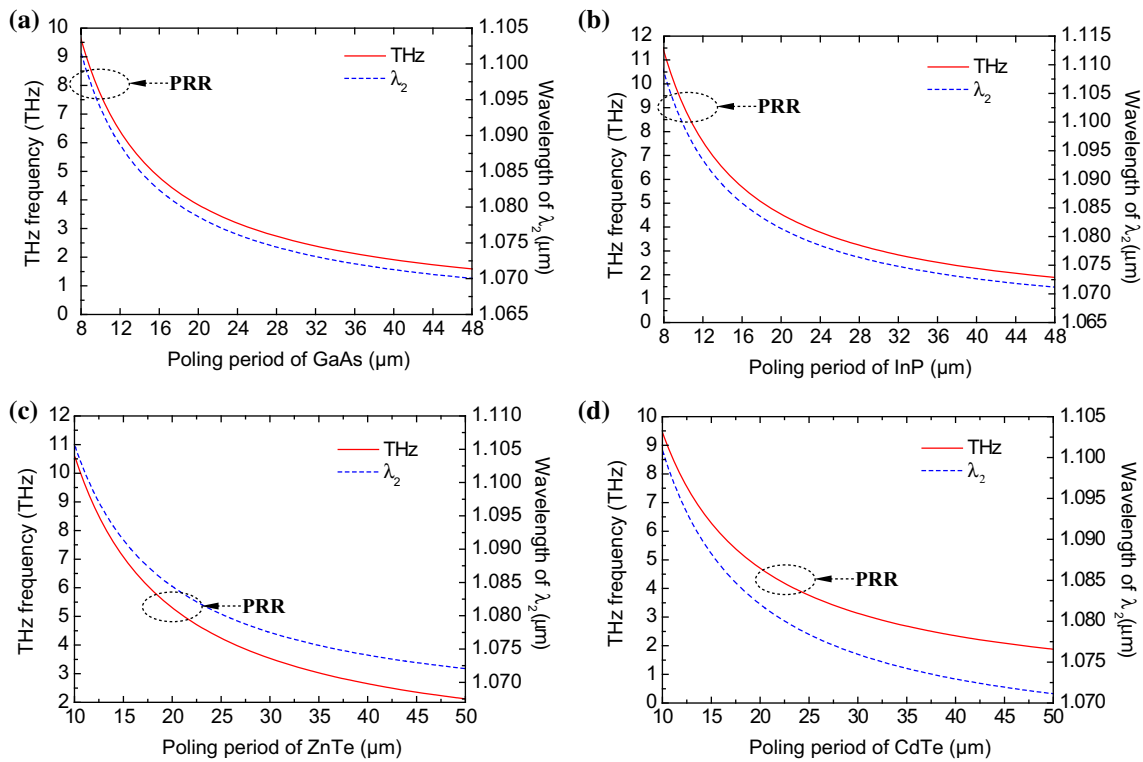

Fig. 4 THz wave frequencies versus the poling period Λ, $\lambda_1 = 1.064$ μm. **a** GaAs, **b** InP, **c** ZnTe, **d** CdTe

of fundamental TE and TM modes in planar waveguide, the absorption at PRR can be efficiently reduced [24].

Conclusion

We explore THz wave generation at PRR of zinc-blende crystal waveguide by DFG with a transverse pumping geometry. It is shown that by using grating vector of periodically inverted crystal, THz wave can be efficiently generated by DFG in the vicinity of PRR. Dramatic enhancement of parametric gain coefficients in the vicinity of PRR can be exploited for improving the output power and extending the frequency bands of THz wave by using a transverse pumping geometry to minimize the propagation path of THz wave within the crystal. THz wave generated from PRR can be realized by tuning the wavelength λ_1 and poling period Λ.

References

1. L. Ho, M. Pepper, P. Taday, Terahertz spectroscopy: signatures and fingerprints. Nat. Photon. **2**, 541–543 (2008)
2. J.F. Federici, B. Schulkin, F. Huang, D. Gary, R. Barat, F. Oliveira, D. Zimdars, THz imaging and sensing for security applications-explosives, weapons, and drugs. Semicond. Sci. Technol. **20**, S266–S280 (2005)
3. J.L. Liu, J.M. Dai, S.L. Chin, X.C. Zhang, Broadband terahertz wave remote sensing using coherent manipulation of fluorescence from asymmetrically ionized gases. Nat. Photon. **4**, 627–631 (2010)
4. T. Kleine-Ostmann, T. Nagatsuma, A review on terahertz communications research. J. Infrared Milli. Terahz. Waves **32**, 143–171 (2011)
5. W. Shi, Y.J. Ding, A monochromatic and high-power THz source tunable in the ranges of 2.7–38.4 μm and 58.2–3540 μm for variety of potential applications. Appl. Phys. Lett. **84**, 1635–1637 (2004)
6. P. Zhao, S. Ragam, Y.J. Ding, I.B. Zotova, X. Mu, H. Lee, S.K. Meissner, H. Meissner, Singly resonant optical parametric oscillator based on adhesive-free-bonded periodically inverted KTiOPO$_4$ plates: terahertz generation by mixing a pair of idler waves. Opt. Lett. **37**, 1283–1285 (2012)
7. Y. Jiang, D. Li, Y.J. Ding, I.B. Zotova, Terahertz generation based on parametric conversion: from saturation of conversion efficiency to back conversion. Opt. Lett. **36**, 1608–1610 (2011)
8. H. Minamide, S. Hayashi, K. Nawata, T. Taira, J. Shikata, K. Kawase, Kilowatt-peak terahertz-wave generation and sub-femtojoule terahertz-wave pulse detection based on nonlinear optical wavelength-conversion at room temperature. J. Infrared Milli. Terahz. Waves **35**, 25–37 (2014)
9. T. Akiba, Y. Akimoto, K. Suizu, K. Miyamoto, T. Omatsu, Evaluation of polarized terahertz waves generated by Cherenkov phase matching. Appl. Opt. **53**, 1518–1522 (2014)
10. T. Tanabe, K. Suto, J. Nishizawa, K. Saito, T. Kimura, Tunable terahertz wave generation in the 3- and 7-THz region from GaP. Appl. Phys. Lett. **83**, 237–239 (2003)
11. Z. Li, P. Bing, S. Yuan, D. Xu, J. Yao, Investigation on terahertz generation at polariton resonance of MgO:LiNbO$_3$ by difference frequency generation. Opt. Laser Technol. **69**, 13–16 (2015)
12. Y.J. Ding, Efficient generation of high-frequency terahertz waves from highly lossy second-order nonlinear medium at polariton resonance under transverse-pumping geometry. Opt. Lett. **35**, 262–264 (2010)
13. Y.H. Avetisyan, Terahertz-wave surface-emitted difference-frequency generation without quasi-phase-matching technique. Opt. Lett. **35**, 2508–2510 (2010)
14. R. Chen, G. Sun, G. Xu, Y.J. Ding, I.B. Zotova, Generation of high-frequency terahertz waves in periodically poled LiNbO$_3$ based on backward parametric interaction. Appl. Phys. Lett. **101**, 111101 (2012)
15. R. Sowade, I. Breunig, C. Tulea, K. Buse, Nonlinear coefficient and temperature dependence of the refractive index of lithium niobate crystals in the terahertz regime. Appl. Phys. B **99**, 63–66 (2010)
16. I. Shoji, T. Kondo, R. Ito, Second-order nonlinear susceptibilities of various dielectric and semiconductor materials. Opt. Quantum Electron. **34**, 797–833 (2002)
17. C. Flytzanis, J. Ducuing, Second-order optical susceptibilities of III–V semiconductors. Phys. Rev. **178**, 1218–1228 (1969)
18. K.L. Vodopyanov, Optical THz-wave generation with periodically-inverted GaAs. Laser Photon. Rev. **2**, 11–25 (2008)
19. C.B. Ebert, L.A. Eyres, M.M. Fejer, J.S. Harris, MBE growth of antiphase GaAs films using GaAs/Ge/GaAs heteroepitaxy. J. Cryst. Growth **201**(202), 187–193 (1999)
20. S. Koh, T. Kondo, M. Ebihara, T. Ishiwada, H. Sawada, GaAs/Ge/GaAs sublattice reversal epitaxy on GaAs (100) and (111) substrates for nonlinear optical devices. Jpn. J. Appl. Phys. **38**, L508–L511 (1999)
21. S.S. Sussman, *Tunable Light Scattering from Transverse Optical Modes in Lithium Niobate*. Stanford University, Microwave Laboratory Report No. 1851 (1970)
22. C.C. Shih, A. Yariv, Quantitative calculation of electro-optic coefficients of diatomic crystals. Phys. Rev. Lett. **44**, 281–284 (1980)
23. I. Shoji, T. Kondo, A. Kitamoto, M. Shirane, R. Ito, Absolute scale of second-order nonlinear-optical coefficients. J. Opt. Soc. Am. B **14**, 2268–2294 (1997)
24. K. Saito, T. Tanabe, Y. Oyama, Widely tunable surface-emitted monochromatic terahertz-wave generation beyond the Reststrahlen band. Opt. Communications **335**, 99–101 (2015)